ARTICLE OPEN ACCESS

Microglia Activation in Basal Ganglia Is a Late Event in Huntington Disease Pathophysiology

Natalia P. Rocha, PhD, Odelin Charron, MSc, Leigh B. Latham, PhD, Gabriela D. Colpo, PhD, Paolo Zanotti-Fregonara, MD, PhD, Meixiang Yu, PhD, Leorah Freeman, MD, PhD, Erin Furr Stimming, MD,* and Antonio L. Teixeira, MD, PhD*

Correspondence
Dr. Rocha
npessoarocha@gmail.com

Neurol Neuroimmunol Neuroinflamm 2021;8:e984. doi:10.1212/NXI.0000000000000984

Abstract

Objective

To define the role played by microglia in different stages of Huntington disease (HD), we used the TSPO radioligand [11C]-ER176 and PET to evaluate microglial activation in relation to neurodegeneration and in relation to the clinical features seen at premanifest and manifest stages of the disease.

Methods

This is a cross-sectional study in which 18 subjects (6 controls, 6 premanifest, and 6 manifest HD gene carriers) underwent a [11C]-ER176 PET scan and an MRI for anatomic localization. Segmentation of regions of interest (ROIs) was performed, and group differences in [11C]-ER176 binding (used to evaluate the extent of microglial activation) were assessed by the standardized uptake value ratio (SUVR). Microglial activation was correlated with ROIs volumes, disease burden, and the scores obtained in the clinical scales. As an exploratory aim, we evaluated the dynamic functions of microglia in vitro, by using induced microglia-like (iMG) cells from peripheral blood monocytes.

Results

Individuals with manifest HD present higher [11C]-ER176 SUVR in both globi pallidi and putamina in comparison with controls. No differences were observed when we compared premanifest HD with controls or with manifest HD. We also found a significant correlation between increased microglial activation and cumulative disease burden, and with reduced volumes. iMG from controls, premanifest HD, and manifest HD patients showed similar phagocytic capacity.

Conclusions

Altogether, our data demonstrate that microglial activation is involved in HD pathophysiology and is associated with disease progression.

*These authors contributed equally to this work as co–senior authors.

From the Mitchell Center for Alzheimer's Disease and Related Brain Disorders (N.P.R.), Department of Neurology, McGovern Medical School, The University of Texas Health Science Center, Houston; Department of Neurology (O.C., L.F.), The University of Texas at Austin; School of Medicine (L.B.L.), University of Washington, Seattle; Neuropsychiatry Program (G.D.C., A.L.T.), Department of Psychiatry and Behavioral Sciences, McGovern Medical School, University of Texas, Houston; Houston Methodist Research Institute and Weill Cornell Medicine (P.Z.-F., M.Y.), TX; and HDSA Center of Excellence at University of Texas Health Science Center at Houston (E.F.S.).

Go to Neurology.org/NN for full disclosures. Funding information is provided at the end of the article.

The Article Processing Charge was funded by the Department of Psychiatry and Behavioral Sciences, UTHealth.

Glossary

3D = 3 dimensional; **CAP** = CAG age product; **HD** = Huntington disease; **IL** = interleukin; **iMG** = induced microglia-like; **IND** = Investigational New Drug Application; **MFI** = median fluorescence intensity; **MMSE** = Mini–Mental State Examination; **PBA-s** = short version of the Problem Behaviors Assessment; **PE** = phycoerythrin; **ROI** = region of interest; **SDMT** = Symbol Digit Modalities Test; **SUVR** = standardized uptake value ratio; **TNF** = tumor necrosis factor; **UHDRS** = Unified HD Rating Scale.

Huntington disease (HD) is an autosomal dominant disease caused by a trinucleotide (CAG) repeat expansion in the huntingtin gene (*HTT*).[1] The toxic gain of function of the expanded mutant huntingtin protein (HTT) seems to be the key event involved in the progressive neuronal dysfunction and neuronal loss, particularly in the striatum and cortex. As a result, individuals with HD classically present with motor dysfunction, cognitive decline, and behavioral disorders.[2] Although the cause of HD is well established, the mechanisms underlying neuronal dysfunction and death are not completely understood. Mutant HTT seems to trigger a pathogenic cascade that includes oxidative stress and immune/inflammatory mechanisms, which are further stimulated by neuronal dysfunction/death. Together, these mechanisms have been regarded as key contributors to the pathophysiology of HD.[3]

Neuroinflammation in HD has been reported since early postmortem studies, which described reactive astrocytes[4,5] and microglial activation[6] in brain regions associated with HD pathogenesis. Inflammatory mechanisms in the CNS are thought to be initiated as compensatory responses against misfolded protein oligomers and/or deposits.[7] On the other hand, inflammatory responses can trigger neuronal damage and thus contribute to disease progression.[8] Noteworthy, the above-mentioned postmortem studies showed that both microglial activation and reactive astrocytosis grades correlate with disease severity.[4-6] These results motivated studies to evaluate neuroinflammation in HD in vivo. In this regard, PET neuroimaging studies have focused on evaluating microglial activation through specific molecular targets in vivo. Microglial activation imaging is currently performed by using PET tracers binding to the 18-kDa translocator protein (TSPO), a mitochondrial protein that is highly expressed in phagocytic inflammatory cells, including activated microglia in the brain and macrophages in the periphery.[9,10] TSPO is expressed at very low levels in the CNS, but its levels are upregulated by activated microglia.[10]

The prototype isoquinoline ligand for TSPO, [11C]-PK11195, has been introduced in the field of molecular brain imaging of microglial activation more than 20 years ago.[9] However, PK11195 shows low specific signal-to-noise ratios, even in clinical conditions in which microglial activation is a prominent and well-established feature.[11] This limitation motivated the development of alternative TSPO PET ligands with better signal-to-noise ratios, such as [11C]-PBR28 and other second-generation ligands.[11] However, other technical issues became evident, mainly the aberrantly low TSPO binding in some individuals due to the single nucleotide polymorphism rs6971. More recently, a series of 4-phenylquinazoline-2-carboxamides lacking allelic sensitivity to the human single nucleotide polymorphism rs6971 has been developed. Noteworthy, [11C]-ER176 (11C-(R)-N-sec-butyl-4-(2-chlorophenyl)-N-methylquinazoline-2-carboxamide), a new analog of [11C]-PK11195,[12] presents higher specific binding when compared with most of the available TSPO binders.[13] Although still sensitive to *TSPO* polymorphism, ER176 allows the inclusion of low-affinity binders because of its high in vivo binding potential.[14] Of note, [11C]-ER176 has a higher specific binding and a smaller intersubject variability compared with [11C]-PBR28, thus resulting in higher statistical power and requiring fewer subjects for clinical studies. Therefore, [11C]-ER176 should be preferred over [11C]-PBR28 for TSPO studies in humans.[15]

To date, 6 studies have used PET neuroimaging with TSPO binders to evaluate microglial activation in HD. Five studies used the first-generation TSPO radiotracer [11C]-PK11195,[16-20] and one used the second-generation TSPO binder, [11C]-PBR28.[21] These studies revealed increased microglial activation in HD gene carriers, which correlated with disease stage and/or severity of symptoms. The available findings indicate that microglial activation is involved in HD pathophysiology and TSPO PET imaging may be a valuable tool to monitor HD progression and therapeutic efficacy of drugs targeting neuroinflammation. However, these indications have yet to be explored. So far, no study has evaluated the use of the novel TSPO tracer, [11C]-ER176, as a marker of microglial activation in HD gene carriers. Therefore, the current study was designed to define the role played by microglia in different stages of HD by using [11C]-ER176 PET. We evaluated microglial activation in HD gene carriers in relation to neurodegeneration and in relation to the clinical features seen at premanifest and manifest stages of the disease. As an exploratory aim, we evaluated the dynamic functions of microglia in vitro, by using induced microglia-like (iMG) cells from human peripheral blood cells.

Methods

Subjects and Clinical Evaluation

This cross-sectional study included 18 subjects: 6 controls, 6 premanifest, and 6 manifest HD gene carriers. The *HTT*

expansion was confirmed by a genotype larger CAG allele ≥36. A movement disorder specialist evaluated all HD gene carriers, and the clinical diagnosis of HD was based on the motor signs certainty, i.e., a Diagnostic Confidence Level of 4 in the Unified HD Rating Scale (UHDRS).[2,22] Patients were recruited from the Huntington Disease Society of America Center of Excellence at UTHealth. Controls were recruited from the local community, comprising a group of people with no history of neurologic or psychiatric disorder. We excluded individuals who have had infectious or autoimmune diseases in activity or who have used anti-inflammatories in the 4 weeks before the study; pregnant or breastfeeding women; and participants with claustrophobia, metal implants incompatible with MRI, previous neurosurgery, or current serious comorbidity (e.g., cancer). Participants' recruitment and study procedures were performed from July 2018 to January 2019.

HD gene carriers completed the UHDRS[22] including the total motor scale, the total functional capacity, and independence scales. The cognitive evaluation included the Mini-Mental State Examination (MMSE),[23] the Symbol Digit Modalities Test (SDMT), the Stroop Interference Test, and the Verbal fluency test.[22] Behavioral symptoms were assessed with the short version of the Problem Behaviors Assessment (PBA-s).[24]

The CAG age product (CAP) score was used to estimate the progression of HD pathology as a function of CAG repeat length and time of exposure to the effects of the expansion.[2] The CAP has been defined as:

$$CAP = AGE \times (CAG - L)/K$$

where AGE is the current age of the individual, CAG is the repeat length, and L and K are constants. L is an estimate of the lower limit of the CAG expansion at which phenotypic expression of the effects of mutant HTT could be observed, and K is a normalizing constant. We used the CAP proposed by Warner and Sampaio,[25] in which L = 30 and K = 6.27, and the CAP will be equal to 100 at the subject's expected age of motor symptoms onset.

Assessment of Microglial Activation In Vivo Using PET

Participants received 1 [11C]-ER176 PET scan on a GE Discovery RX PET/CT scanner. Subjects were scanned at rest. An IV line was placed in the antecubital fossa of the arm. Subjects were placed supine on the camera table with their head firmly secured using a thermoplastic facemask. Attenuation correction CT was performed before PET acquisition. Vital signs were obtained before administration of [11C]-ER176 and at the end of the scan. All subjects received a single IV bolus of about 20 mCi of [11C]-ER176 in 10 mL (injected mass dose <10 μg), and PET data were acquired for 90 minutes. Subjects were observed during scanning, and no earlier determination was warranted. Bladder voiding was encouraged to reduce bladder radiation exposure after PET scanning.

For the purpose of anatomic localization, the participants also underwent a whole-brain MRI scan on a 3T Phillips Ingenia scanner using an 8-channel head coil. The MRI protocol included a 3-dimensional (3D) T1-weighted sequence magnetization-prepared gradient echo, repetition time = 8,100 ms, time to echo = 3.7 milliseconds, voxel size 0.94 × 0.94 × 1.5 mm, and 170 slices. PET frames were aligned for motion correction, and the regional time-activity curves were obtained after segmentation with the automated anatomic labeling–merged atlas implemented in the PNEURO module of PMOD 3.8 (PMOD Technologies).[15] Time-activity curves were averaged from 60 to 90 minutes and normalized over that of the whole cerebellum (standardized uptake value ratio [SUVR]), following the methodology described by Lyoo et al.[26]

In terms of analysis, cortical (frontal, cingulate, occipital, temporal, parietal, and insular cortices) and subcortical (thalamus, caudate, putamen, pallidum, hippocampus, and amygdala) regions of interest (ROIs) were selected. Cortical reconstruction and segmentation of the selected ROIs were performed with the recon-all pipeline from FreeSurfer v5.3.0 image analysis suite[27] on the 3DT1 image. The PET parametric map was then registered onto the FreeSurfer processed T1 image using ITK-SNAP[28] in a semiautomatic way. Averaged [11C]-ER176 SUVR and the associated ROI volumes were then extracted from each ROI using FreeSurfer.

In Vitro Evaluation of the Dynamic Functions of Microglia

The same individuals subjected to the PET/MRI scans (N = 18, N = 6 individuals per group) were subjected to a blood drawn. Ten milliliters of blood were collected by venipuncture in vacuum tubes containing heparin on the same day of the PET scan. Monocytes were used to generate iMG cells, as previously described.[29] Briefly, peripheral blood mononuclear cells were isolated by Ficoll gradient centrifugation and plated at a density of 4×10^5 cells/mL. After overnight incubation, nonadherent cells were removed and the adherent cells (mainly monocytes) were cultured with granulocyte-macrophage colony-stimulating factor (10 ng/mL) and interleukin (IL)-34 (100 ng/mL) for 14 days to develop iMG cells. Microglial characterization was evaluated through morphologic and phenotypical changes observed in the fluorescence microscopy, using CX3CR1/CCR2 double staining.

Phagocytosis was examined by fluorescent microscopy and flow cytometry using the Phagocytosis Assay Kit (Cayman Chemical, Ann Arbor, MI). At day 14, phycoerythrin (PE)-conjugated beads were added to the media (1:250) for 24 hours. Cells were observed under the fluorescence microscope and then harvested by nonenzymatic cell dissociation solution (Sigma-Aldrich, St. Louis, MO) and cell lifter. The cells were washed and acquired using a BD FACSJazz cytometer (BD Biosciences, San Jose, CA). Flow cytometry data were analyzed using FlowJo V10 software (Tree Star, Ashland, OR).

Table Demographic and Clinical Characteristics of Premanifest HD Gene Carriers and Manifest Patients With HD Included in This Study

Variable	Controls (N = 6)	HD gene carriers		*p* Value
		Premanifest HD (N = 6)	Manifest HD (N = 6)	
Age, y, mean ± SD (median)	43.28 ± 8.79 (43)	38.15 ± 7.18 (35)	50.75 ± 11.55 (51)	0.121[a]
Sex, female, n (%)	5 (83)	4 (67)	6 (100)	0.301[b]
Educational level, y, mean ± SD (median)	16.42 ± 4.32 (17.5)	15.83 ± 4.45 (14.5)	14.67 ± 3.33 (13.5)	0.598[a]
***TSPO* genotype, n (%)**				
Thr147/Thr147	0	0	0	
Ala147/Thr147	2 (33)	3 (50)	2 (33)	0.792[b]
Ala147/Ala147	4 (67)	3 (50)	4 (67)	
CAP score	—	**74.88 ± 10.27**	**115.09 ± 8.88**	**0.002**[c]
CAG repeats (larger), mean ± SD (median)	—	42.50 ± 1.87 (42.5)	44.67 ± 2.42 (44)	0.180[c]
UHDRS-TMS, mean ± SD (median)	—	**3.67 ± 3.56 (3)**	**30.83 ± 2.31 (31)**	**0.002**[c]
UHDRS-TFC, mean ± SD (median)	—	**12.50 ± 1.23 (13)**	**7.83 ± 1.84 (7)**	**0.004**[c]
Independence scale	—	**97.50 ± 6.12 (100)**	**84.17 ± 8.61 (85)**	**0.015**[c]
SDMT (total correct), mean ± SD (median)	**54.50 ± 7.84 (54)**	**54.17 ± 9.15 (57.5)**	**30.67 ± 10.19 (33.5)**	**0.004**[d]
Verbal fluency test (category), no. of correct responses in 1 min, mean ± SD (median)	**23.83 ± 3.92 (24)**	**21.67 ± 4.03 (21)**	**11.00 ± 5.25 (10.5)**	**0.008**[e]
Stroop Interference Test, no. of correct responses, mean ± SD (median)	43.83 ± 13.29 (44.5)	40.50 ± 5.99 (40.5)	28.67 ± 16.26 (25.5)	0.091[a]
MMSE, mean ± SD (median)	28.67 ± 1.86 (29)	28.83 ± 0.98 (28.5)	26.60 ± 3.21 (28)	0.138[a]
PBA-s domain scores, mean ± SD (median)				
Depression	4.00 ± 5.55 (2)	6.17 ± 5.46 (6.5)	7.17 ± 10.96 (2.5)	0.871[a]
Irritability/aggression	1.33 ± 2.34 (0.5)	2.83 ± 3.25 (2)	2.33 ± 2.66 (2)	0.845[a]
Psychosis	0.00 ± 0.00 (0)	0.17 ± 0.41 (0)	0.00 ± 0.00 (0)	0.368[a]
Apathy	1.00 ± 0.89 (1)	2.50 ± 3.56 (0.5)	3.83 ± 4.40 (3.5)	0.546[a]
Executive function	**0.00 ± 0.00 (0)**	**4.50 ± 4.46 (4)**	**4.67 ± 3.50 (5)**	**0.024**[f]

Abbreviations: HD = Huntington disease; MMSE = Mini-Mental State Examination; PBA-s = short version of the Problem Behaviors Assessment; SDMT = Symbol Digit Modalities Test; TFC = total functional capacity; TMS = total motor score; UHDRS = Unified Huntington's Disease Rating Scale.
Significant values are highlighted in bold.
[a] Kruskal-Wallis test.
[b] Pearson χ^2 test.
[c] Mann-Whitney test.
[d] Kruskal-Wallis followed by Dunn multiple comparisons test: (controls = premanifest HD) < manifest HD.
[e] Kruskal-Wallis followed by Dunn multiple comparisons test: post hoc: (controls = premanifest HD) > manifest HD.
[f] Kruskal-Wallis followed by Dunn multiple comparisons test: post hoc: (controls = premanifest HD) > manifest HD.

Secretion of inflammatory cytokines (tumor necrosis factor [TNF]-α, IL-6, and IL-1β) during phagocytosis was measured from culture supernatant using a Multiplex Immunoassay, following the manufacturer instructions (Bio-Rad Laboratories, Hercules, CA). Briefly, the samples and standards were incubated with magnetic microspheres covalently coupled with antibodies directed against the desired biomarker (i.e., TNFα, IL-1β, and IL-6). After a series of washes to remove unbound protein, a biotinylated detection antibody was added to create a sandwich complex (similar to that of a sandwich ELISA). The final detection complex was formed with the addition of streptavidin-PE conjugate. PE served as a fluorescent indicator. Data from standards and samples and a standard curve were acquired in a Bio-Plex 200

Figure 1 Microglial Activation in HD

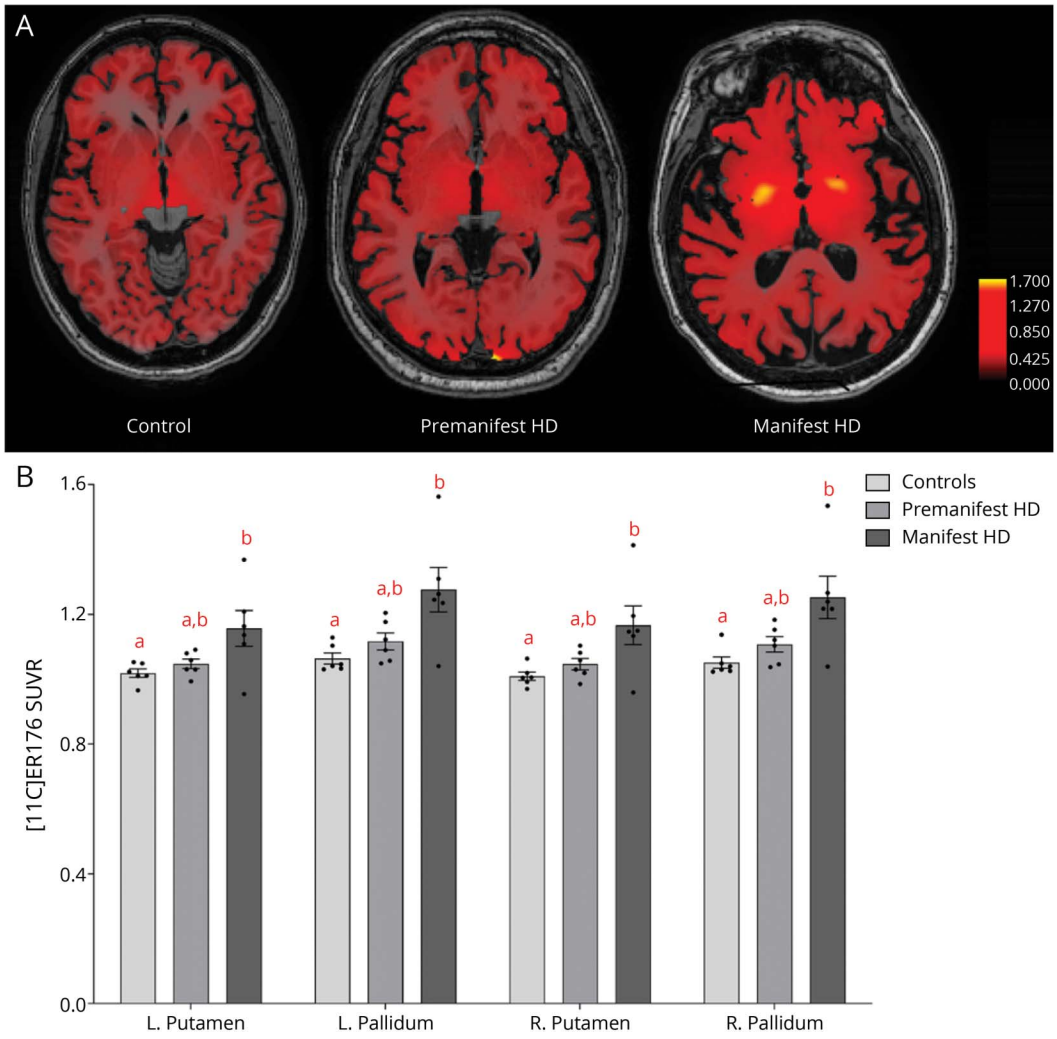

(A) PET image showing increased [11C]-ER176 standardized uptake value ratio (SUVR) in bilateral putamina and pallidi of a patient with manifest HD in comparison with a control. Note that there is no visible difference in [11C]-ER176 SUVR for the premanifest HD gene carrier (central image). (B) Group comparisons in left (L.) and right (R.) putamina and pallidi. Significant differences between groups are indicated by different letters (Kruskal-Wallis test followed by Dunn multiple comparisons test). Horizontal bars show the mean and the standard error of the mean. Data from other regions of interest are shown in figure e-1 (links.lww.com/NXI/A459). HD = Huntington disease.

Reader and analyzed in a Bio-Plex Manager Software, which presented data as median fluorescence intensity (MFI). The cytokine concentrations in the samples were calculated based on a standard curve in which the MFI values obtained from the standard were plotted against the known concentrations (in picograms per milliliter). Cytokine levels (in picograms per milliliter) were measured in the supernatant 24 hours after bead exposure or 24 hours of culture without any stimulus (baseline condition), and the values were corrected by protein levels (in milligrams per milliliter) in the cell lysates using the Pierce BCA Protein Assay Kit (ThermoFisher Scientific, Waltham, MA). The final results are provided in pg/mg.

DNA Polymorphism Genotyping

Peripheral blood mononuclear cells were used for DNA extraction using the QIAamp DNA Blood Mini Kit (Qiagen, Hilden, Germany) and subsequent genotyping for the rs6971 polymorphism (Ala147Thr) in the *TSPO* gene (TaqMan assay ID: C_2512465_20; Thermo Fisher Scientific). Allele Ala147 was linked to Vic, and allele Thr147 was linked to FAM. PCRs were performed in QuantStudio 7 Flex Real-Time PCR system (Life Technologies/Thermo Fisher Scientific).

Statistical Analysis

Association between dichotomous variables was assessed with the χ^2 test. Our limited sample size made it difficult to ascertain data distribution, and therefore, nonparametric tests were used. Comparisons between the 3 groups were made by the Kruskal-Wallis test. When appropriate, post hoc analyses were used to determine significant differences between pairs of groups (Dunn Multiple Comparison Test). The Mann-Whitney test was used for 2-group

Figure 2 Microglial Activation in HD Is Associated With Disease Burden

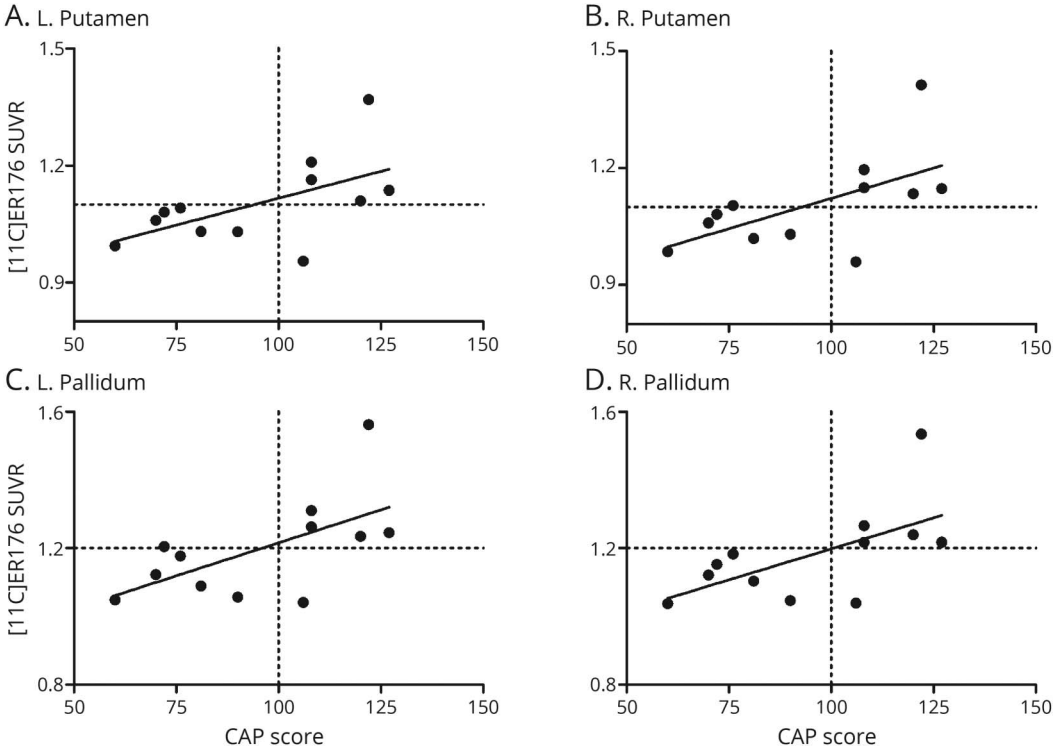

Among HD gene carriers (premanifest and manifest HD), a higher CAP score (a proxy for cumulative disease burden) was significantly associated with higher [11C]-ER176 standardized uptake value ratio (SUVR) in the (A) left putamen (ρ = 0.664, p = 0.018), (B) left pallidum (ρ = 0.657, p = 0.020), (C) right putamen (ρ = 0.671, p = 0.017), and (D) right pallidum (ρ = 0.734, p = 0.007). Note the 2 clusters in [11C]-ER176 SUVR, composed of premanifest HD gene carriers (CAP <100) and manifest patients with HD (CAP >100). CAP = CAG age product; HD = Huntington's disease.

comparisons (premanifest HD vs manifest HD). Spearman correlations were performed to examine the relationship between [11]C-ER176 SUVR in the ROIs significantly different between groups and (1) CAP score; (2) volume in the same ROIs; and (3) scores in the clinical scales. All statistical tests were 2 tailed and were performed using a significance level of $\alpha = 0.05$. Statistical analyses were performed using SPSS software version 26.0 and GraphPad Prism version 5.0.

Standard Protocol Approvals, Registrations, and Patient Consents

All subjects provided written informed consent before admission to the study. The Research Ethics Committees of UTHealth and Houston Methodist Research Institute approved this study.

An Investigational New Drug Application (IND) was submitted, and authorization was obtained from the Food and Drug Administration to use [11C]-ER176 as a PET Imaging agent in this study (IND 139220).

Data Availability

The raw data not provided in the article will be made available by the authors at the request of other investigators for purposes of replicating procedures and results.

Results

Clinical Evaluation and *TSPO* Genotyping

Demographic and clinical characteristics of participants included in this study are shown in the table. There was no significant difference between controls, premanifest HD gene carriers and patients with HD regarding age, sex, and educational level. As expected, patients with manifest HD presented a higher CAP score and worse scores in the scales that evaluated motor symptoms severity, functional capacity, and independence in comparison with premanifest HD (table). The age at clinical diagnosis was 47.67 ± 10.35 years for the patients with manifest HD. Premanifest HD gene carriers had a mean of 12.98 ± 6.17 years before the predicted clinical diagnosis of HD. The 3 groups presented similar performance on the MMSE. Patients with the clinical diagnosis of HD presented worse performance on the SDMT and verbal fluency test in comparison with premanifest and control subjects. Controls, individuals with premanifest HD, and patients with HD presented similar scores in the PBA-s subscales, except for executive function, in which HD gene carriers (both premanifest and manifest HD) scored worse than controls, evidencing that those problems are present before clinical diagnosis of HD (table).

The groups presented similar distribution of *TSPO* genotype (table). Individuals with genotype Ala147/Ala147 were classified as high-affinity binders and those with genotype

Figure 3 Microglial Activation Is Associated With Brain Atrophy

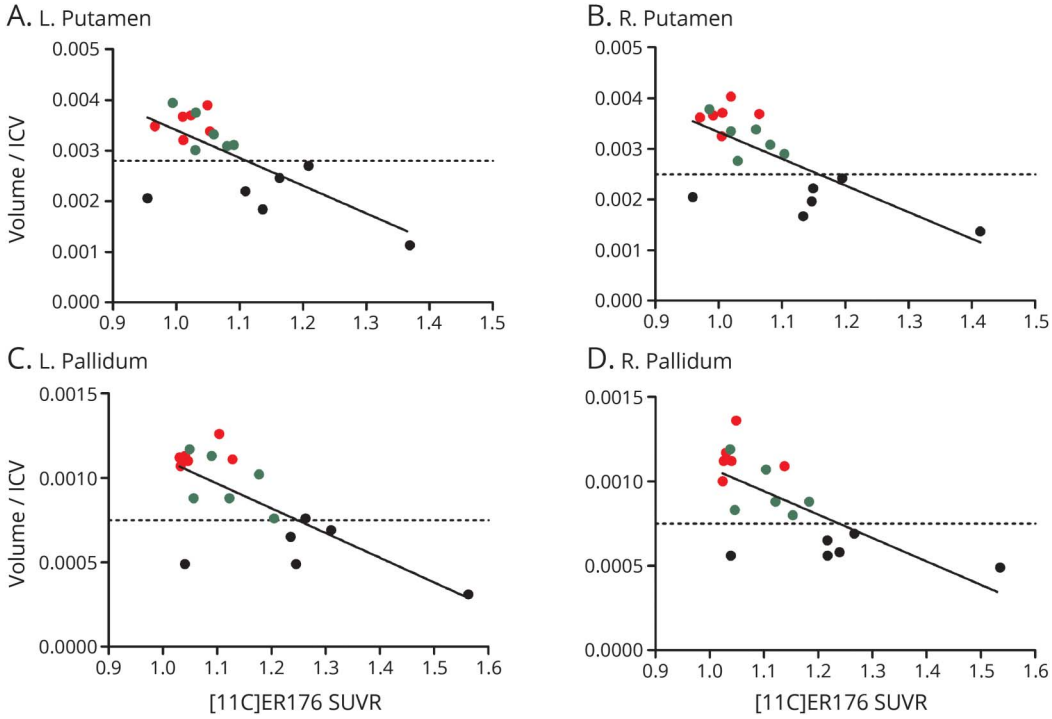

Increased microglial activation is associated with decreased volume in putamen and pallidus. Controls are displayed in red dots, premanifest HD gene carriers in green dots, and manifest HD in black dots. A higher [11C]-ER176 standardized uptake value ratio (SUVR) was associated with a decreased volume in the (A) left putamen ($\rho = -0.569$, $p = 0.014$), (B) left pallidum ($\rho = -0.591$, $p = 0.010$), (C) right putamen ($\rho = -0.601$, $p = 0.008$), and (D) right pallidum ($\rho = -0.686$, $p = 0.002$). ICV = intracranial volume. The dashed line was placed to emphasize the 2 clusters composed of controls + premanifest HD and manifest HD gene carriers. HD = Huntington disease.

Ala147/Thr147 as mixed affinity. None of our patients presented the genotype Thr147/Thr147 (low-affinity binders). Because the groups presented comparable distribution of *TSPO* genotype (table) and the outcome parameter was SUVR, which minimizes genotype differences, no correction for genotype-related binding affinity was performed.

In Vivo Assessment of Microglial Activation

Patients with HD demonstrate higher [11C]-ER176 SUVR in both the left and right globi pallidi and putamina in comparison with controls. These differences were not significant when we compared premanifest HD gene carriers with patients with HD or controls (figure 1 and figure e-1, links.lww.com/NXI/A459). These results indicate increased microglial activation in the putamina and globi pallidi of patients with manifest HD. We found no differences between different *TSPO* genotypes on [11C]-ER176 SUVR when controlling for HD diagnosis (data not shown).

Among HD gene carriers (premanifest and manifest HD), a higher CAP score was significantly associated with higher [11C]-ER176 SUVR in the left putamen ($\rho = 0.664$, $p = 0.018$), left pallidum ($\rho = 0.657$, $p = 0.020$), right putamen ($\rho = 0.671$, $p = 0.017$), and right pallidum ($\rho = 0.734$, $p = 0.007$) (figure 2). Corroborating these findings, increased [11C]-ER176 SUVR was associated with decreased volume in the same ROIs (figure 3).

In Vitro Evaluation of the Dynamic Functions of Microglia

We confirmed that the iMG cells have the immunophenotype of microglial cells, such as $CX3CR1_{high}/CCR2_{low}$, and a typical (i.e., ramified) morphology (figure 4). The iMG cells express dynamic functions such as phagocytosis and secretion of inflammatory cytokines, making them a valuable tool to assess microglial functioning.[30] The phagocytosis assay demonstrated that iMG cells obtained from controls, premanifest HD, and HD patients (figure 5, A–C) showed similar phagocytic capacity (figure 5E). Secretion of inflammatory cytokines (TNFα, IL-6, and IL-1β) during phagocytosis was measured from culture supernatant. As shown in figure 5F, although iMG cells from controls, premanifest HD, and patients with HD increased the production of the evaluated cytokines during phagocytosis, the values were significant only for TNFα in controls and manifest HD (figure 5F).

Discussion

By using [11C]-ER176 PET, we verified that patients with HD have increased microglial activation in basal ganglia structures that are involved in HD pathophysiology, i.e., putamina and globi pallidi. In addition, we found that

Figure 4 Inducing Microglia-Like Cells From Human Peripheral Blood Monocytes

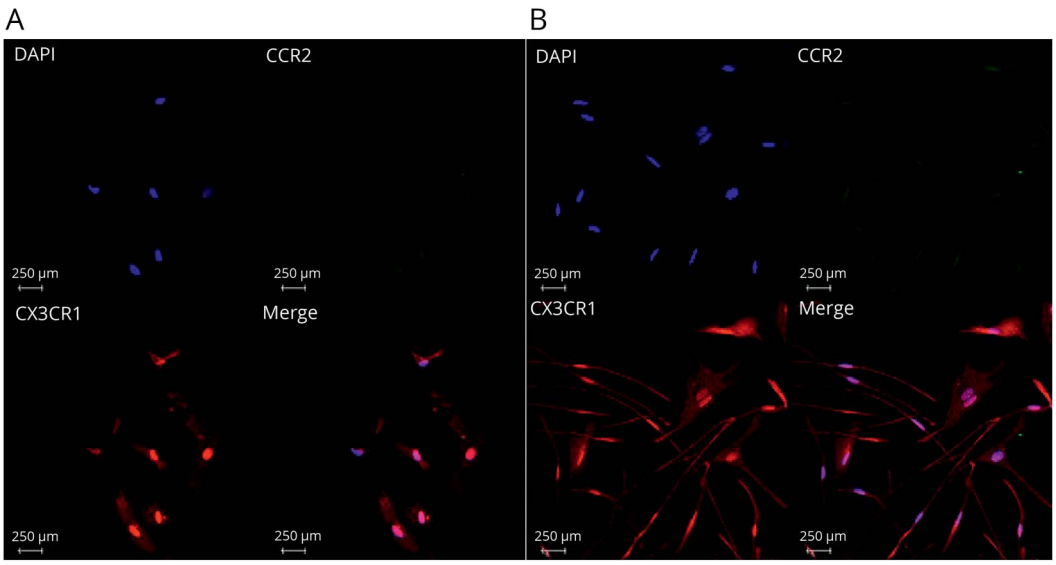

Peripheral blood monocytes were cultured for 14 days in conventional conditions (A) or with GM-CSF and IL-34, resulting in induced microglia like cells that exhibit microglia-like morphology and increased CX3CR1/CCR2 ratio (B).

premanifest HD gene carriers demonstrate [11C]-ER176 SUVRs comparable to controls, suggesting that microglial activation is a later process in HD pathophysiology, becoming evident only after the onset of motor symptoms (figure 1). Supporting these findings, we reported a significant correlation between increased microglial activation and higher CAP scores, a proxy for cumulative disease burden (figure 2). Moreover, increased microglial activation in putamina and pallidi was significantly associated with reduced volumes in the same ROIs (figure 3). Individuals with manifest HD presented a significant decrease in the cortical volume in comparison with controls (data not shown). Despite already presenting cortical atrophy, manifest HD individuals do not have increased microglial activation in the cortex (figure 1). The only areas displaying increased microglia activation are those that are known to be affected early in HD pathophysiology. Because PET scans require individuals to be still for 90 minutes, our sample did not include patients in moderate/late stages of HD. Whether increased microglia activation will occur in the cortex later in the HD course is yet to be determined. Altogether, our data demonstrate that microglial activation is involved in HD pathophysiology and is associated with disease progression (as demonstrated by the CAP score and atrophy in basal ganglia structures). Our findings support the conclusions of previous research that reported that microglial activation correlates with disease severity, contributing to the ongoing neuronal degeneration in HD.[16]

HD has been regarded as an important model to study neurodegenerative diseases as it is caused by a single genetic mutation and is amenable to predictive genetic testing, enabling the study of patients before clinical diagnosis.[2] In this study, we assessed microglial activation not only in patients with HD, but also in premanifest HD gene carriers with a mean of 13 years before the predicted onset of clinical symptoms. Our results corroborate the view that microglial activation is unlikely to be the initiating event in HD, but may contribute to neuronal death through multiple pathways.[31]

Similar to other neurodegenerative diseases, the mechanisms underlying selective neuronal dysfunction and death in HD are still uncertain. In addition to impairment in systems for handling abnormal proteins, other metabolic pathways and mechanisms might contribute to neurodegeneration and progression of HD, such as mitochondrial dysfunction, impaired neurotrophic support, oxidative stress, and inflammatory/immune mechanisms.[8,32,33] In the current study, we described a significant increase in microglial activation in regions of neurodegeneration in HD, suggesting that this process is related to the disease pathophysiology and not to random premorbid events. Accordingly, postmortem studies reported significant microglial activation in regions implicated in HD pathogenesis.[4,6] The fact that we found significant microglial activation in patients with manifest HD (but not in premanifest HD gene carriers) in comparison with controls, suggests that this event occurs in response or concomitantly to neuronal death. This assumption is further corroborated by the finding of significant associations between microglial activation and ROI volumes as well as CAP scores. Here again, our data are corroborated by postmortem findings, in which the number of activated microglia in the striatum and cortex correlated with neuronal loss, confirming the hypothesis that neuroinflammation may be elicited by degenerating neurons.[6]

Figure 5 Phagocytosis by Induced Microglia-Like (iMG) Cells

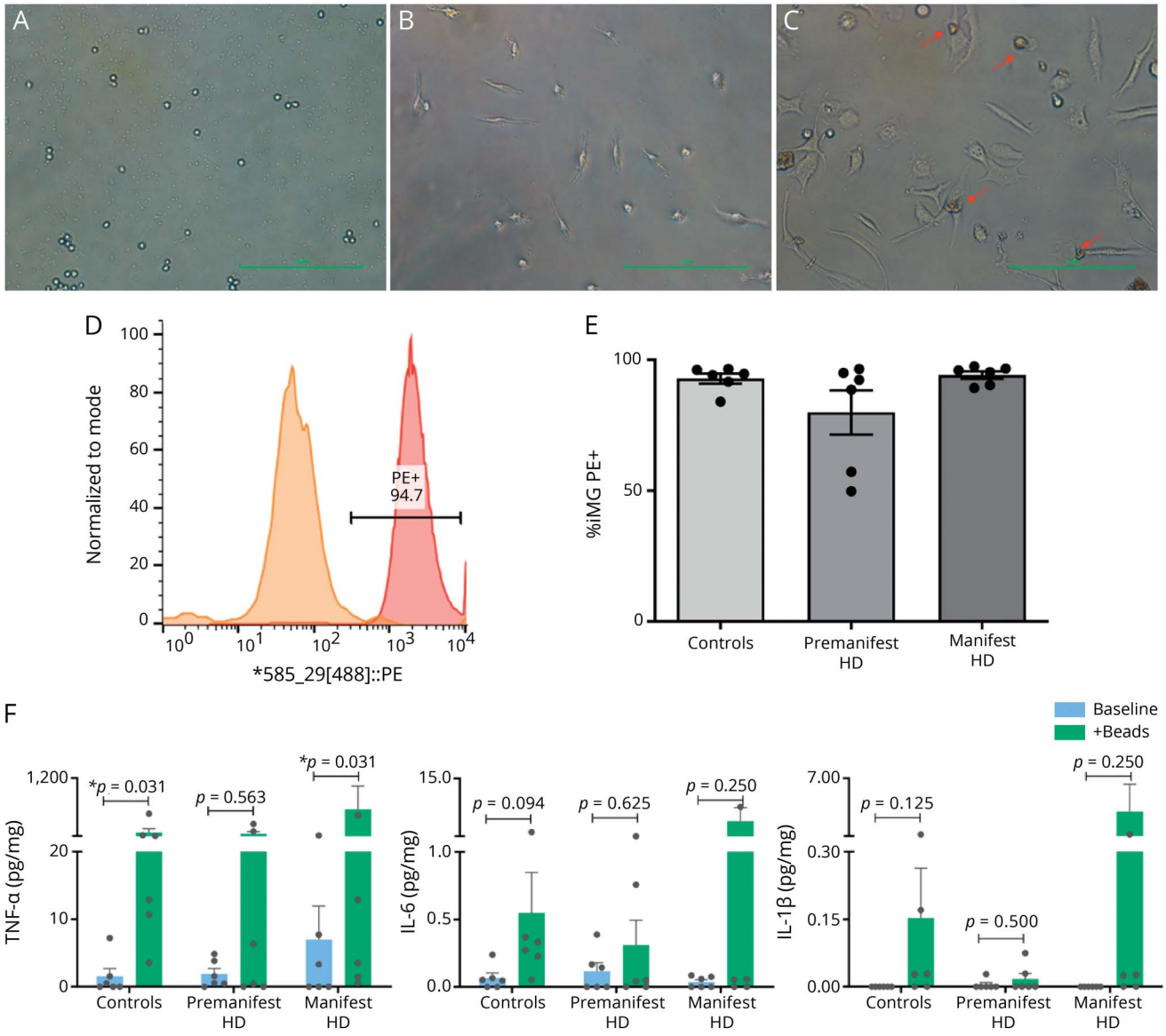

Peripheral blood monocytes (day 1, panel A) were cultured for 14 days with GM-CSF and IL-34, resulting in iMG cells (day 14, panel B). Phagocytosis was assessed by exposing iMG cells to PE-conjugated (1:250) beads (panel C) for 24 hours. The iMG cells showed the ability of phagocytosis with morphological changes (C). The read arrows show PE-conjugated beads phagocytosed by iMG cells. After washing beads out, cells were acquired in a flow cytometer and analyzed. iMG were first gated by forward/side scatter (not shown). PE uptake was analyzed as shown in (D): orange (left) histogram shows the cells without beads (negative control); red (right) histogram shows the cells that phagocytosed to the PE-conjugated beads. Quantification is shown in (E). iMG from controls, premanifest HD, and HD patients showed similar phagocytic capacity (no significant difference found at the Kruskal-Wallis test). (F) Cytokine production during phagocytosis. iMG cells were incubated with PE-conjugated beads (1:250) for 24 hours. Supernatant was collected, and cytokines were analyzed by multiparametric assay. Cytokine levels (in picograms per milliliter) were corrected by protein levels (in milligrams per milliliter). Although iMG cells from controls, premanifest HD, and patients with HD increased the production of the evaluated cytokines during phagocytosis, the values were significant only for TNFα in controls and manifest HD (*p* values are provided in the figure, Wilcoxon matched-pairs signed-rank test). Scale bar (A–C) = 1.0 mm. Horizontal bars (E and F) show the mean and the standard error of the mean. HD = Huntington disease; PE = phycoerythrin; TNF = tumor necrosis factor.

Neuroinflammation elicited by neuronal death can be at first regarded as a positive event as it promotes clearance of cell debris. However, inflammatory mechanisms contribute to neurodegeneration, and dying neurons further activate inflammatory responses, resulting in a vicious cycle of inflammation and neuronal death.[34] Therefore, inflammatory responses, although essential for tissue homeostasis, can contribute to neuronal injury. As neural tissues have a restricted cell renewal and regenerative capacity, the CNS is extremely vulnerable to uncontrolled and/or chronic immune and inflammatory processes.[34] Interestingly enough, our data corroborate this hypothesis as we observed increased microglial activation later in the HD course (i.e., manifest HD) reinforcing the idea that neuroinflammation contributes to disease progression rather than to disease onset. Activated microglia releases proinflammatory mediators, including

cytokines and reactive oxygen species, which, in turn, will also contribute to neuronal death and further microglial activation.[34] We observed an increase in cytokine release (especially TNFα) following a phagocytic stimulus in our in vitro experiments. In line with our findings, postmortem studies have also reported increased levels of inflammatory cytokines in brain samples of patients with HD in comparison with controls.[35,36] It is worth mentioning that cytokine release is a microglial reaction to a proinflammatory challenge, and under controlled conditions (such as the iMG cultures), phagocytosis is a noninflammatory function of microglia. A proinflammatory stimulus would be needed to appropriately assess differences in cytokine release between controls, premanifest HD, and manifest HD iMG cultures.

The current study used a novel PET tracer for TSPO, [11C]-ER176, to assess microglial activation in HD. By using [11C]-PK11195 PET, studies have shown a significant increase in microglial activation in the striatum of patients with HD[16] as well as in premanifest HD gene carriers[18] compared with controls. In both studies, [11C]-PK11195 binding significantly correlated with disease severity, as measured by decreased [11C]-raclopride (a marker of dopamine D2 and D3 receptor availability) binding in the striatum.[16,18] Similar results were described in the hypothalamus.[17] Later, the same work group used a multimodal imaging approach combining MRI and PET analyses, and worsening in atrophy evaluated by MRI was accompanied by a reduction in [11C]-raclopride and an increase in [11C]-PK11195 bindings in patients with HD. In premanifest HD, increased level of microglial activation in the associative striatum and in the regional network associated with cognition correlated with 5-year probability of HD onset.[19] More recently, increased microglial activation in the somatosensory cortex (as evaluated through [11C]-PK11195 binding) was associated with higher levels of IL-1β, IL-6, IL-8, and TNFα produced by stimulated peripheral blood monocytes from premanifest HD gene carriers.[20,37] Although these studies provided valuable information about neuroinflammation in HD, indicating microglial activation even in premanifest subjects, their results should be interpreted with caution. The poor signal-to-background ratio of first-generation TSPO radiotracers poses important limitations to the analyses. The ratio of specific to nonspecific binding of [11C]-PK11195 in human brain has been reported to be as low as 0.2.[38,39] As an attempt to mitigate this problem, a recent study used the second-generation TSPO tracer, [11C]-PBR28, to evaluate microglial activation in HD.[21] Of interest, the results were similar to ours, i.e., increased levels of [11C]-PBR28 binding in the putamina and pallidi of HD gene carriers (which included 7 manifest patients with HD and only 1 person with premanifest HD) in comparison with controls. Of note, the results of the single premanifest subject were midway between controls and the remaining patients, suggesting that microglial activation was associated with disease progression.[21] The authors did confirm that [11C]-PBR28 provides a high signal-to-background ratio, an important feature required for the analysis at the individual level and within individual brain regions. An important limitation of [11C]-PBR28 and other second-generation TSPO radioligands is that they have varying degrees of sensitivity to the single nucleotide polymorphism rs6971 in the *TSPO* gene.[40] [11C]-ER176 has unique advantages over the other TSPO binders, being the only known TSPO radioligand that allows the inclusion of low-affinity binders. The binding of ER176 in low-affinity binders was found to be comparable to that for PBR28 in high-affinity binders. Moreover, ER176 was proven to be the only radioligand not contaminated by radiometabolites accumulating in the brain.[14]

Our findings must be interpreted while taking into account the limitations of the study, which include the relatively small sample size and the cross-sectional design. The cross-sectional design prevented the assessment of microglial activation in the context of disease progression and development of motor and nonmotor symptoms. In addition, the use of an objective method to measure striatal degeneration (e.g., [11C]-raclopride PET) would provide more accurate information about striatal neuron dysfunction/death. Regarding the in vitro experiments, the use of a proinflammatory challenge (other than the beads added for the phagocytosis assay) in our experiments would provide valuable information on cytokines release by iMG from the different groups. It is worth mentioning the strengths of the study that include the use of a unique TSPO ligand, [11C]-ER176, the enrollment of both premanifest and manifest subjects, and the exploratory investigation of microglia activity.

In conclusion, our findings strengthen the evidence that microglial activation is associated with HD pathophysiology. Microglial activation is unlikely to be the initiating event in HD. Yet, it may exacerbate neuronal dysfunction and neuronal death, thus contributing to disease progression. It is important to refine our understanding of the more specific immune/inflammatory mechanisms that are involved in HD and in neurodegeneration. This may foster the development of new therapeutic interventions to halt the progression of HD and other neurodegenerative diseases.

Acknowledgment

The authors acknowledge and thank all of the volunteers that participated in this study and are indebted to their families for their magnificent support. They also thank the staff from the UTHealth McGovern Medical School 3T MRI Center and from the Houston Methodist Research Institute Translational Imaging Core Facilities, especially Vips Patel and Kim M. Doan, for their skilled technical support; Dr. Gabriel Fries for his assistance with the genotyping analyses; and the team members of the HDSA Center of Excellence at UTHealth.

Study Funding

This study was funded by the HD Human Biology Project—Huntington's Disease Society of America (HDSA). E. Furr Stimming receives research funding from Roche/Genetech, Vaccinex, Cures Within Reach, HDSA, Uniqure, and CHDI Foundation.

Disclosure

The authors report no disclosures relevant to the manuscript. Go to Neurology.org/NN for full disclosures.

Publication History

Received by *Neurology: Neuroimmunology & Neuroinflammation* September 9, 2020. Accepted in final form January 20, 2021.

Appendix Authors

Name	Location	Contribution
Natalia P. Rocha, PhD	The Mitchell Center for Alzheimer's Disease and Related Brain Disorders, Department of Neurology, McGovern Medical School, The University of Texas Health Science Center, Houston	Designed and conceptualized the study; major role in the acquisition of data; analyzed the data; and drafted the manuscript for intellectual content
Odelin Charron, MS	Department of Neurology, The University of Texas at Austin	Major role in data analysis
Leigh B. Latham, PhD	School of Medicine, University of Washington, Seattle	Major role in the acquisition of data
Gabriela D. Colpo, PhD	Neuropsychiatry Program, Department of Psychiatry and Behavioral Sciences, McGovern Medical School, University of Texas, Houston	Major role in the acquisition of data
Paolo Zanotti-Fregonara, MD, PhD	Houston Methodist Research Institute and Weill Cornell Medicine, TX	Major role in the study design and the acquisition of data
Meixiang Yu, PhD	Houston Methodist Research Institute and Weill Cornell Medicine, TX	Major role in the acquisition of data
Leorah Freeman, MD, PhD	Department of Neurology, The University of Texas at Austin	Major role in the study design, data analysis and interpretation, and the acquisition of data
Erin Furr Stimming, MD	HDSA Center of Excellence at University of Texas Health Science Center at Houston	Major role in the study design and acquisition of data, interpreted the data; and revised the manuscript for intellectual content
Antonio L. Teixeira, MD, PhD	Neuropsychiatry Program, Department of Psychiatry and Behavioral Sciences, McGovern Medical School, University of Texas, Houston	Major role in the study design and acquisition of data, interpreted the data; and revised the manuscript for intellectual content

References

1. The Huntington's Disease Collaborative Research Group. A novel gene containing a trinucleotide repeat that is expanded and unstable on Huntington's disease chromosomes. Cell 1993;72:971–983.
2. Ross CA, Aylward EH, Wild EJ, et al. Huntington disease: natural history, biomarkers and prospects for therapeutics. Nat Rev Neurol 2014;10:204–216.
3. Soulet D, Cicchetti F. The role of immunity in Huntington's disease. Mol Psychiatry 2011;16:889–902.
4. Myers RH, Vonsattel JP, Paskevich PA, et al. Decreased neuronal and increased oligodendroglial densities in Huntington's disease caudate nucleus. J Neuropathol Exp Neurol 1991;50:729–742.
5. Vonsattel JP, Myers RH, Stevens TJ, Ferrante RJ, Bird ED, Richardson EP Jr. Neuropathological classification of Huntington's disease. J Neuropathol Exp Neurol 1985;44:559–577.
6. Sapp E, Kegel KB, Aronin N, et al. Early and progressive accumulation of reactive microglia in the Huntington disease brain. J Neuropathol Exp Neurol 2001;60:161–172.
7. Ciccocioppo F, Bologna G, Ercolino E, et al. Neurodegenerative diseases as proteinopathies-driven immune disorders. Neural Regen Res 2020;15:850–856.
8. Rocha NP, Ribeiro FM, Furr-Stimming E, Teixeira AL. Neuroimmunology of Huntington's disease: revisiting evidence from human studies. Mediators Inflamm 2016;2016:8653132.
9. Vowinckel E, Reutens D, Becher B, et al. PK11195 binding to the peripheral benzodiazepine receptor as a marker of microglia activation in multiple sclerosis and experimental autoimmune encephalomyelitis. J Neurosci Res 1997;50:345–353.
10. Papadopoulos V, Baraldi M, Guilarte TR, et al. Translocator protein (18kDa): new nomenclature for the peripheral-type benzodiazepine receptor based on its structure and molecular function. Trends Pharmacol Sci 2006;27:402–409.
11. Cumming P, Burgher B, Patkar O, et al. Sifting through the surfeit of neuroinflammation tracers. J Cereb Blood Flow Metab 2018;38:204–224.
12. Zanotti-Fregonara P, Zhang Y, Jenko KJ, et al. Synthesis and evaluation of translocator 18 kDa protein (TSPO) positron emission tomography (PET) radioligands with low binding sensitivity to human single nucleotide polymorphism rs6971. ACS Chem Neurosci 2014;5:963–971.
13. Ikawa M, Lohith TG, Shrestha S, et al. 11C-ER176, a radioligand for 18-kDa translocator protein, has adequate sensitivity to robustly image all three affinity genotypes in human brain. J Nucl Med 2017;58:320–325.
14. Fujita M, Kobayashi M, Ikawa M, et al. Comparison of four (11)C-labeled PET ligands to quantify translocator protein 18 kDa (TSPO) in human brain: (R)-PK11195, PBR28, DPA-713, and ER176-based on recent publications that measured specific-to-non-displaceable ratios. EJNMMI Res 2017;7:84.
15. Zanotti-Fregonara P, Pascual B, Veronese M, et al. Head-to-head comparison of (11)C-PBR28 and (11)C-ER176 for quantification of the translocator protein in the human brain. Eur J Nucl Med Mol Imaging 2019;46:1822–1829.
16. Pavese N, Gerhard A, Tai YF, et al. Microglial activation correlates with severity in Huntington disease: a clinical and PET study. Neurology 2006;66:1638–1643.
17. Politis M, Pavese N, Tai YF, Tabrizi SJ, Barker RA, Piccini P. Hypothalamic involvement in Huntington's disease: an in vivo PET study. Brain 2008;131:2860–2869.
18. Tai YF, Pavese N, Gerhard A, et al. Microglial activation in presymptomatic Huntington's disease gene carriers. Brain 2007;130:1759–1766.
19. Politis M, Pavese N, Tai YF, et al. Microglial activation in regions related to cognitive function predicts disease onset in Huntington's disease: a multimodal imaging study. Hum Brain Mapp 2011;32:258–270.
20. Politis M, Lahiri N, Niccolini F, et al. Increased central microglial activation associated with peripheral cytokine levels in premanifest Huntington's disease gene carriers. Neurobiol Dis 2015;83:115–121.
21. Lois C, Gonzalez I, Izquierdo-Garcia D, et al. Neuroinflammation in Huntington's disease: new insights with (11)C-PBR28 PET/MRI. ACS Chem Neurosci 2018;9:2563–2571.
22. Huntington Study Group. Unified Huntington's Disease Rating Scale: reliability and consistency. Mov Disord 1996;11:136–142.
23. Folstein MF, Folstein SE, McHugh PR. "Mini-mental state". A practical method for grading the cognitive state of patients for the clinician. J Psychiatr Res 1975;12:189–198.
24. McNally G, Rickards H, Horton M, Craufurd D. Exploring the validity of the short version of the Problem Behaviours Assessment (PBA-s) for Huntington's disease: a rasch analysis. J Huntingtons Dis 2015;4:347–369.
25. Warner JH, Sampaio C. Modeling variability in the progression of Huntington's disease: a novel modeling approach applied to structural imaging markers from TRACK-HD. CPT Pharmacometrics Syst Pharmacol 2016;5:437–445.
26. Lyoo CH, Ikawa M, Liow JS, et al. Cerebellum can serve as a pseudo-reference region in Alzheimer disease to detect neuroinflammation measured with PET radioligand binding to translocator protein. J Nucl Med 2015;56:701–706.
27. Reuter M, Schmansky NJ, Rosas HD, Fischl B. Within-subject template estimation for unbiased longitudinal image analysis. Neuroimage 2012;61:1402–1418.
28. Yushkevich PA, Piven J, Hazlett HC, et al. User-guided 3D active contour segmentation of anatomical structures: significantly improved efficiency and reliability. Neuroimage 2006;31:1116–1128.
29. Ohgidani M, Kato TA, Setoyama D, et al. Direct induction of ramified microglia-like cells from human monocytes: dynamic microglial dysfunction in Nasu-Hakola disease. Sci Rep 2014;4:4957.
30. Ohgidani M, Kato TA, Kanba S. Introducing directly induced microglia-like (iMG) cells from fresh human monocytes: a novel translational research tool for psychiatric disorders. Front Cell Neurosci 2015;9:184.
31. Kim SU, de Vellis J. Microglia in health and disease. J Neurosci Res 2005;81:302-313.
32. Ross CA, Tabrizi SJ. Huntington's disease: from molecular pathogenesis to clinical treatment. Lancet Neurol 2011;10:83–98.
33. Chitnis T, Weiner HL. CNS inflammation and neurodegeneration. J Clin Invest 2017;127:3577–3587.

34. Rocha NP, de Miranda AS, Teixeira AL. Insights into neuroinflammation in Parkinson's disease: from biomarkers to anti-inflammatory based therapies. Biomed Res Int 2015;2015:628192.
35. Silvestroni A, Faull RL, Strand AD, Moller T. Distinct neuroinflammatory profile in post-mortem human Huntington's disease. Neuroreport 2009;20:1098–1103.
36. Bjorkqvist M, Wild EJ, Thiele J, et al. A novel pathogenic pathway of immune activation detectable before clinical onset in Huntington's disease. J Exp Med 2008;205:1869–1877.
37. Politis M, Lahiri N, Niccolini F, et al. Corrigendum to "Increased central microglial activation associated with peripheral cytokine levels in premanifest Huntington's disease gene carriers" [Neurobiol. Dis. 83 (2015) 115-121]. Neurobiol Dis 2017;98:162.
38. Kropholler MA, Boellaard R, Schuitemaker A, Folkersma H, van Berckel BN, Lammertsma AA. Evaluation of reference tissue models for the analysis of [11C](R)-PK11195 studies. J Cereb Blood Flow Metab 2006;26:1431–1441.
39. Turkheimer FE, Edison P, Pavese N, et al. Reference and target region modeling of [11C]-(R)-PK11195 brain studies. J Nucl Med 2007;48:158–167.
40. Kreisl WC, Jenko KJ, Hines CS, et al. A genetic polymorphism for translocator protein 18 kDa affects both in vitro and in vivo radioligand binding in human brain to this putative biomarker of neuroinflammation. J Cereb Blood Flow Metab 2013;33:53–58.